

NUMERICAL SIMULATION OF THE FLOW AROUND FOUR EQUAL-DISTANCE CYLINDERS IN CROSS-FLOW USING THE VORTEX METHOD WITH TURBULENCE MODELING

Luiz Antonio Alcântara Pereira

Instituto de Engenharia Mecânica, UNIFEI, CP. 50, Itajubá, Minas Gerais, 37500-903, Brasil
luizantp@unifei.edu.br

Miguel Hiroo Hirata

FAT/UERJ, Campus Regional de Resende, Estrada Resende-Riachuelo, Resende, Rio de Janeiro, Brasil
hirata@fat.uerj.br

Abstract. *The discrete vortex method is used to the investigation of interference effects of four circular cylinders in a square configuration at high Reynolds number. The vortex method is also modified to take into account the sub grid-scale phenomena; a second-order velocity structure function model is adapted to the lagrangian scheme. The vorticity generated on the bodies surface is discretized and is numerically simulated using discrete Lamb vortices. The aerodynamics forces are obtained using an integral equation derived from the pressure Poisson equation, which was first developed for a single body. Results for the numerical simulation around four cylinders are presented and comparisons are made with experimental results available in the literature.*

Keywords: *vortex method, panels method, sub-scale model, interference, aerodynamics loads.*

1. Introduction

Investigation of the characteristics of flow around simple configurations of objects is helpful for understanding the flow around more complex and larger-scale structures. In many cases of engineering practices, objects often appear in the form of groups, e.g. groups of buildings, chimneys, stacks, chemical reaction-towers, supports of off-shore platform, etc.

Numerous investigations have been made of the flow past circular cylinder configurations. The flow around a bluff body is complex and many of its aspects can be considered as open questions, deserving additional investigations. Much of this complexity is associated to the phenomena occurring inside the boundary layer which strongly interacts with the near field viscous wake. To overcome the difficulties of the analysis much effort is required. The development of new techniques and a fresh approach to the solution of the problems are urgently needed. Due the mutual interference between cylinders at close proximity, the aerodynamics characteristics, such as fluctuating lift and drag forces, vortex-shedding patterns and fluctuating pressure distributions, for each member of a group are completely different from isolated ones. When a cylinder is placed in the wake of another in cross-flow its unsteady loading becomes dependent not only on the flow activities in its wake, but also on those in the wake of the upstream cylinder.

Zdravkovich (1977) and Ohya *et al.* (1989) presented an extensive review of the state of knowledge of flow across two cylinders in various arrangements. Previous investigations of tandem configurations by Biermann and Herrnstein (1933), Kostic and Oka (1972), Novak (1974), Zdravkovich and Pridden (1975, 1977), Okajima (1979), Igarashi (1981, 1984), Hiwada *et al.* (1982), Arie *et al.* (1983), Jendrzeczyk and Chen (1986) have revealed considerable complexity in fluid dynamics as the spacing or gap between the cylinders is changed.

The interference phenomena are highly non-linear and there are many discrepant points in previous works. Arie *et al.* (1983) pointed out that fluctuation in drag force acting both cylinders is weakly dependent on spacing. On the other hand, Igarashi (1981) reported that the fluctuation in pressure associated with fluctuation in aerodynamics forces (lift and drag) acting on a downstream cylinder is strongly dependent on gap between the cylinders. Alam *et al.* (2003) presented an experimental study in which fluctuating lift and drag forces acting on the cylinders was measured. In their work they elucidated the discrepant points and clarified the flow patterns over the cylinders.

Recently, the Vortex Method was employed by Alcântara Pereira and Hirata (2006a) to simulate the vortex-shedding flow from two tandem cylinders in cross-flow; the aerodynamic characteristics are investigated at a Reynolds number of 6.5×10^4 and comparisons are made with experimental results presented by Alam *et al.* (2003). As the simulations showed, the numerical results obtained are in overall good agreement with the experimental results used for comparison, especially in the simulations for the upstream cylinder. Some discrepancies observed in the determination of the aerodynamics loads for the downstream cylinder may be attributed to errors in the treatment of vortex element moving away from a solid surface. Because every vortex element has different strength of vorticity, it will diffuse to different location in the flow field. It seems impossible that every vortex element will move to same ε -layer normal to the solid surface. In the present method all nascent vortices were placed into the cloud through a same displacement normal to the panels. The turbulence modeling was taking into account using a second-order velocity structure function model (Alcântara Pereira *et al.*, 2002).

Kareem *et al.* (1998) presented an experimental study of the interference effects between two and three cylinders of finite height immersed in a turbulent boundary layer at subcritical Reynolds number utilizing a pneumatic averaging manifold system to measure the fluctuating force at various levels.

Lam *et al.* (2001a) employed the Vortex Method to simulate flows around four equi-spaced cylinders. The surface of the each cylinder was represented by straight-line panels with a point vortex located at the control point; the coalescence of vortices when they are too close to each other was introduced, and the pressure on the airfoil surface was calculated according to the inviscid flow analysis. A comparison of the aerodynamics loads obtained with the experimental results by Lam and Fang (1995) showed a better agreement in the drag direction. A more sophisticated scheme is required to obtain better prediction on pressure and force characteristics. He and Su (1994) showed that the results for the pressure calculation could be improved by considering the nonlinear acceleration terms.

Alcântara Pereira and Hirata (2006b) employed the Vortex Method to simulate the interference effects for a group of finite cylinders. The interference phenomena are highly non-linear and at present beyond a reliable theoretical or numerical analysis. The main feature of their vortex code is to simulate numerically the two-dimensional, incompressible, unsteady flow around of pipe clusters: (a) for two pipes, for three-pipes clusters, (c) for regular square multiple clusters, (d) and for irregular multi-pipe clusters. The Vortex Method is used to simulate the macro scale phenomena, however, the effect of small scale is not considered.

The Vortex Method have been developed and applied for analysis of complex, unsteady and vortical flows in relation to problems in a wide range of industries, because they consist of simple algorithm based on physics of flow (Kamemoto, 2004). In this method, the vorticity in the fluid region is numerically simulated using a cloud of discrete vortices with a viscous core. To simulate the vorticity at the solid surfaces, nascent vortices are generated there at each time step of the simulation. In order to take care of the convection and the diffusion of the vorticity one makes use of the convection-diffusion splitting algorithm; accordingly the convection of the vortices in the cloud is carried out independently of the diffusion for each time step of the simulation. This is in essence the foundation of the Vortex Method (e.g. references Chorin, 1973; Sarpkaya, 1989; Sethian, 1991; Kamemoto, 1994; Lewis, 1999; Ogami, 2001 and Alcântara Pereira *et al.*, 2002). Please note that with the Lagrangian formulation a grid for the spatial discretization of the fluid region is not necessary. Thus, special care to handle numerical instabilities associated to high Reynolds numbers is not needed. Also, the attention is only focused on the regions of high activities, which are the regions containing vorticity; on the contrary, Eulerian schemes consider the entire domain independent of the fact that there are sub-regions where less important, if any, flow activity can be found. With the Lagrangian tracking of the vortices, one need not take into account the far away boundary conditions. This is of important in the wake regions (which is not negligible in the flows of present interest) where turbulence activities are intense and unknown, a priori.

In the present paper, the Vortex Method is employed to simulate the vortex-shedding flow from four cylinders in a square configuration; the turbulence modeling is taking into account using a second-order velocity structure function model (Alcântara Pereira *et al.*, 2002). The aerodynamic characteristics are investigated at a Reynolds number of 1.3×10^4 and comparisons are made with experimental results presented by Lam and Fang (1995).

2. Mathematical formulation

Consider the incompressible fluid flow of a Newtonian fluid around four-pipe clusters an unbounded two-dimensional region. Figure 1 shows the incident flow, defined by free stream speed U and the domain Ω with boundary $S = S_1 \cup S_2 \cup S_3 \cup S_4 \cup S_5$; being S_1, S_2, S_3 and S_4 the cylinders surface and S_5 the far away boundary.

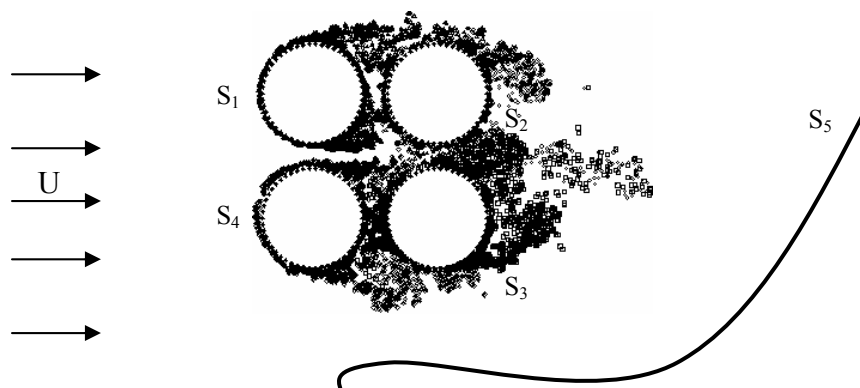


Figure 1. Flow around four equi-spaced circular cylinders.

As the Newtonian fluid flow is supposed to be incompressible the governing equations are (Alcântara Pereira *et al.*, 2002)

$$\frac{\partial \bar{u}_i}{\partial x_i} = 0, \quad i=1, 2 \quad (1)$$

$$\frac{\partial \bar{u}_i}{\partial t} + \bar{u}_j \frac{\partial \bar{u}_i}{\partial x_j} = -\frac{1}{\rho} \frac{\partial \bar{p}}{\partial x_i} + \frac{\partial}{\partial x_j} \left[(v + v_t) \bar{S}_{ij} \right] \quad (2)$$

where the summation convention applies. The above governing was filtered ($u_i = \bar{u}_i + u_i'$, u_i' denotes the fluctuation field), v is the molecular viscosity, v_t is the eddy-viscosity of the fluid, ρ is the fluid density, \bar{S}_{ij} is the deformation tensor of the filtered field and p is the pressure.

The large structures are governed by Eq. (2) and the eddy-viscosity assumption (Boussinesq's hypothesis) is used to model the sub-grid scale tensor $T_{ij} = \bar{u}_i u_j - \bar{u}_i \bar{u}_j$ (Smagorinsky, 1963).

The impermeability and no-slip conditions on the cylinders surface are written as

$$\mathbf{u}_n = \mathbf{u} \cdot \mathbf{e}_n = 0 \quad (3)$$

$$\mathbf{u}_\tau = \mathbf{u} \cdot \mathbf{e}_\tau = 0 \quad (4)$$

\mathbf{e}_n and \mathbf{e}_τ being, respectively, the unit normal and tangential vectors. One assumes that, far away, the perturbation caused by the bodies fades as

$$|\mathbf{u}| \rightarrow U \quad \text{at } S_\infty. \quad (5)$$

In order to take into account the local activities of turbulence, Métais and Lesieur (1992) considered that the small scales may not be too far from isotropy and proposed to use the local kinetic-energy spectrum $E(k_c)$ at the cut-off wave number (k_c) to define the eddy-viscosity v_t . Using a relation proposed by Batchelor (1967), the local spectrum at k_c is calculated with a local second-order velocity structure function \bar{F}_2 of the filtered field (Lesieur and Métais, 1996)

$$\bar{F}_2(\mathbf{x}, \Delta, t) = \overline{\|\bar{\mathbf{u}}(\mathbf{x}, t) - \bar{\mathbf{u}}(\mathbf{x} + \mathbf{r}, t)\|^2}_{\|\mathbf{r}\|=\Delta}. \quad (6)$$

From the Kolmogorov spectrum the eddy-viscosity can be written as a function of \bar{F}_2

$$v_t(\mathbf{x}, \Delta, t) = 0.104 C_k^{-2/3} \Delta \sqrt{\bar{F}_2(\mathbf{x}, \Delta, t)} \quad (7)$$

where $C_k = 1.4$ is the Kolmogorov constant.

The great computational advantage of above formulation over Smagorinsky (1963) model is that in Eq. (6) the notion of velocity fluctuations (differences of velocity) is used instead of the rate of deformation (derivatives). The velocities $\mathbf{u}(\mathbf{x} + \mathbf{r})$ are calculated over the surface of a sphere of radius Δ . In this paper this formulation is adapted for 2D problems and to take advantage of the Lagrangian scheme (Alcântara Pereira *et al.*, 2002). Therefore, for each vortex of the cloud, one has

$$\bar{F}_2 = \frac{1}{N_v} \sum_{i=1}^{N_v} \|\mathbf{u}(\mathbf{x}) - \mathbf{u}(\mathbf{x} + \mathbf{r}_i)\|^2 \left(\frac{\sigma_0}{r_i} \right)^{2/3}. \quad (8)$$

In Eq. (8), N_v is the number of discrete vortices of the cloud found in the region defined by distances $r_1 = 0.1\sigma_0$ and $r_2 = 2.0\sigma_0$ from the centre of the reference vortex. A correction $(\sigma_0/r_i)^{2/3}$ is necessary due to the fact that the N_v vortices are not located at equal distance from the center of the reference vortex.

In the numerical simulation, consider a point vortex of the cloud, which is located at point L. The value of the velocity structure function \bar{F}_2 which measures the turbulence manifestations is statistically sound only if the neighborhood of L is sufficiently populated with other point vortices. After some numerical experiments with the flow

around a circular cylinder, it was assumed that this happens if $N_v / A > 100$, where N_v is the number of point vortices in the region, of area A , defined by two circumferences centered in L and with radius $r_1 = 0.1\sigma_0$ and $r_2 = 2.0\sigma_0$.

It is also worth to observe that the turbulence is essentially a 3-D phenomenon and yet one is modeling it using a 2-D approach; obviously it is then assumed 2-D turbulence. With this procedure one are still left with important turbulence aspects and the final results are also improved. The use of 2-D turbulence may explain some numerical results that depart from the experimental values.

3. The discrete vortex method with turbulence model

From Eq. (1) and Eq. (2) one can write the non-dimensional vorticity equation in two dimensions as

$$\frac{\partial \omega}{\partial t} + \mathbf{u} \cdot \nabla \omega = \frac{1 + v_t^*}{Re} \nabla^2 \omega \quad (9)$$

As can be seen the equations are non-dimensionalized in terms of U and b (a reference length). The Reynolds number is defined by

$$Re = \frac{bU}{\nu} \quad (9a)$$

where ω is the only component of the vorticity vector; the dimensionless time is b/U and

$$v_t^* = \frac{\nu_t}{\nu} \quad (10)$$

The vorticity equation carries information about the convection and the diffusion of vorticity. For the numerical simulation, the viscous splitting algorithm, first proposed by Chorin (1973), says that, in each time step, these process are governed by

$$\frac{\partial \omega}{\partial t} + \mathbf{u} \cdot \nabla \omega = 0, \text{ convection process} \quad (11)$$

$$\frac{\partial \omega}{\partial t} = \frac{1 + v_t^*}{Re} \nabla^2 \omega, \text{ diffusion process.} \quad (12)$$

Convection is governed by Eq. (11) and the velocity field is given by

$$\mathbf{u} - i\mathbf{v} = \mathbf{u}_{\text{main stream}} + \mathbf{u}_{\text{cylinders}} + \mathbf{u}_{\text{vortex cloud}} \quad (13)$$

Here, u and v are the x and y components of the velocity vector \mathbf{u} and $i = \sqrt{-1}$. The first term in the right hand sides is the contribution of the incident flow; the second term in the right hande sides is the summation of M integral terms comes from the vortices panels distributed on cylinders surface. The third term is associated to the velocity induced by the cloud of N free vortices; it represents the vortex-vortex interactions.

The process of vorticity generation is carried out from Eq. (4), so as to satisfy the no-slip condition. According to the discussion above the panels method guaranties that the no-slip condition is satisfied in each straight-line element, or panel, at pivotal point. At each instant of the time M new vortices are created a small distance ε of the cylinders surface along the radial direction. This procedure yields an algebraic system of M equations and M unknowns (the density of the vortices).

In this paper, an improvement was also introduced in the convective step of the simulation; by using the anti symmetry property of the vortex-vortex velocity induction, the computational effort was reduced; this is an important feature, since the vortex-vortex velocity induction calculation is the most time consuming part of the simulation.

The Lamb vortex model is used to represent the vortex cloud, whose mathematical expression for the induced velocity of the k th vortex with strength $\Delta\Gamma_k$ in the circumferential direction u_{θ_k} is given by (Mustto *et al.*, 1998)

$$u_{\theta k} = \frac{\Delta \Gamma_k}{2\pi r} \left\{ 1 - \exp \left[-5.02572 \left(-\frac{r}{\sigma_0} \right)^2 \right] \right\} \quad (14)$$

where σ_0 is the radius of the vortex core, which is updated according to

$$\sigma_0 = 4.48364 \sqrt{\frac{\Delta t (1 + v_t^*)}{\text{Re}}} \quad (15)$$

Each vortex particle distributed in the flow field is followed during numerical simulation according to the Adams-Bashforth second-order formula (Ferziger, 1981)

$$z(t + \Delta t) = z(t) + [1.5u(t) - 0.5u(t - \Delta t)]\Delta t + \xi \quad (16)$$

in which z is the position of a vortex particle, Δt is the time increment and ξ is the diffusion displacement.

It is important to observe that the viscous diffusion of vorticity, governed by Eq. (12), was taken care of by using the random walk method, a molecular (laminar) diffusion process (Lewis, 1999). In our approach the variation of the core radius is only performed locally where the flow is turbulent, that means an additional (turbulent) diffusion process.

The pressure calculation starts with the Bernoulli function, defined by Uhlman (1992) as

$$Y = p + \frac{u^2}{2}, \quad u = |\mathbf{u}| \quad (17)$$

Kamemoto (1993) used the same function and starting from the Navier-Stokes equations was able to write a Poisson equation for the pressure. This equation was solved using a finite difference scheme. Here the same Poisson equation was derived and its solution was obtained through the following integral formulation (Shintani and Akamatsu, 1994)

$$H\bar{Y}_i - \int_{S_{1,2,3,4}} \bar{Y} \nabla G_i \cdot \mathbf{e}_n dS = \iint_{\Omega} \nabla G_i \cdot (\mathbf{u} \times \boldsymbol{\omega}) d\Omega - \frac{1}{\text{Re}} \int_{S_{1,2,3,4}} (\nabla G_i \times \boldsymbol{\omega}) \cdot \mathbf{e}_n dS \quad (18)$$

Here H is 1.0 inside the flow (at domain Ω) and is 0.5 on the boundaries S_1, S_2, S_3 and S_4 . $G_i = (1/2\pi) \log R^{-1}$ is the fundamental solution of Laplace equation, R being the distance from i th vortex element to the field point.

It is worth to observe that this formulation is specially suited for a Lagrangian scheme because it utilizes the velocity and vorticity field defined at the position of the vortices in the cloud. Therefore it does not require any additional calculation at mesh points. Numerically, Eq. (18) is solved by mean of a set of simultaneous equations for pressure Y_i . The pressure coefficient on a panel control point i is calculated according to $C_{p_i} = 1 + Y_i$.

4. Discussion and results

The numerical simulations were restricted to the interference effects between two and four cylinders in a cross uniform flow. Here, l is the spacing between circular cylinders center, and b is the cylinders diameter. Table 1 presents all cases studied for two circular cylinders in a tandem arrangement at a subcritical Reynolds number of 6.5×10^4 without turbulence modeling (Teixeira da Silveira *et al.*, 2005). In the calculations, each cylinders surface was represented by fifty ($M=50$) straight-line vortex panels with constant density. All runs were performed with 600 time steps of magnitude $\Delta t=0.05$. The time increment was evaluated according to $\Delta t=2\pi k/M$, $0 < k \leq 1$ (Musto *et al.*, 1998). In each time step the nascent vortices were placed into the cloud through a displacement $\varepsilon = \sigma_0 = 0.03b$ normal to the panels. The aerodynamics forces and pressure distributions computations starts at $t=15$. The aerodynamics force coefficients are calculated through the integration of the pressure coefficient distribution on the each cylinders surface.

Within the results presented in Table 1, is observed a disagreement of the numerical results to the experimental results (Alam *et al.*, 2003) of cases III, IV and VII on the time-averaged drag coefficient, C_D , of the downstream cylinder. The mean drag coefficients of the downstream cylinder are much higher than the experimental values and, therefore, do not reflect a good simulation of the flow. The differences encountered in the comparison of the numerical results with the experimental results are attributed mainly the inherent three-dimensionality of the real flow for such a value of the Reynolds number, which is not modeled in the present simulation. A purely two-dimensional computation of such flow must produce higher values for the drag coefficient, as obtained for our simulation.

No attempts to simulate the flow for M greater than 50 were made since the operation count of the algorithm is proportional to the square of N . As M increases N also tends to increase, and the computation becomes expensive.

Experiments (Alam *et al.*, 2003) were conducted in a low-speed, closed-circuit wind tunnel with a test section of 0.6 m height, 0.4 m width, and 5.4 m length. The level of turbulence in the working section was 0.19%. The cylinders used as test models were made of brass and were each 49 mm in diameter. The geometric blockage ratio and aspect ratio at the test section were 8.1% and 8.2, respectively. None of the results presented were corrected for the effects of wind-tunnel blockage.

Table 1. Comparison of the mean drag coefficient with experimental results without turbulence modeling, for $Re=6.5 \times 10^4$.

Case	l/b	Upstream cylinder		Downstream cylinder	
		C_D^+	C_D^*	C_D^+	C_D^*
I	0.1	1.0953	1.1500	-0.5697	-0.5447
II	0.5	---	0.9866	-0.3884	-0.2997
III	1.0	1.0531	1.3664	-0.2366	0.1130
IV	2.0	0.9866	1.3434	-0.1345	0.3652
V	3.5	1.2612	1.3677	0.2766	0.4613
VI	4.0	1.2319	1.4174	0.2661	0.3015
VII	8.0	1.2040	1.4324	0.3604	0.8693

⁺ Experimental results (Alam *et al.*, 2003)

^{*} Present calculation without turbulence modeling

As the simulations show, the numerical results obtained are in overall good agreement with the experimental results used for comparison, especially in the simulations for the upstream cylinder. Some discrepancies observed in the determination of the aerodynamics loads for the downstream cylinder for spacing $l/b=1.0$, $l/b=2.0$ and $l/b=8.0$ may be attributed to errors in the treatment of vortex element moving away from a solid surface. Because every vortex element has different strength of vorticity, it will diffuse to different location in the flow field. It seems impossible that every vortex element will move to same ε -layer normal to the solid surface. In the present method all nascent vortices were placed into the cloud through a displacement $\varepsilon = \sigma_0 = 0.03b$ normal to the panels.

The sub-grid turbulence modeling is of significant importance for the numerical simulation. The results of this analysis (Alcântara Pereira and Hirata, 2006a), taking into account the sub-grid turbulence modeling are presented in Table 2.

Table 2. Comparison of the mean drag coefficient with experimental results with turbulence modeling, for $Re=6.5 \times 10^4$.

Case	l/b	Upstream cylinder		Downstream cylinder	
		C_D^+	C_D^*	C_D^+	C_D^*
I	0.1	1.0953	0.8782	-0.5697	-0.9447
II	0.5	---	0.8751	-0.3884	-0.2225
III	1.0	1.0531	1.0607	-0.2366	0.1142
IV	2.0	0.9866	1.1687	-0.1345	0.5315
V	3.5	1.2612	1.2034	0.2766	0.3202
VI	4.0	1.2319	1.1551	0.2661	0.5609
VII	8.0	1.2040	1.1962	0.3604	0.5224

⁺ Experimental results (Alam *et al.*, 2003)

^{*} Present calculation with turbulence modeling

As it can be seen, qualitatively, the behaviour of the results with sub-grid scale modeling is more regular, showing already the improvements obtained with turbulence modeling. The sub-grid scale modeling improved the results but the drag coefficient is still high especially for downstream cylinder for spacing $l/b=1.0$ and $l/b=2.0$.

More investigations are needed and one can imagine that with the use of more panels (and therefore more free vortices in the cloud) the results tend to be in closer agreement with the experiments.

The graphs for the variation with time of the lift and drag coefficients and pressure distribution can be viewed in Alcântara Pereira and Hirata (2006a, b).

Numerical simulations of the flow around four cylinders in a square configurations have been carried out at sub-critical Reynolds number ($Re=1.3 \times 10^4$) and several spacing ratios. However, typical results for four equal size cylinders at spacing ratios $l/b=1.5$ and $l/b=4.0$, and with flow incident angles that vary from 0° (normal configuration) to 45° (rotate square configuration) have been investigated. The reason for this choice of parameters is due the experimental

data obtained at subcritical Reynolds numbers ($2.0 \times 10^2 - 1.3 \times 10^4$) can be found in Lam and Lo (1992) Lam and Fang (1995) and Lam *et al.* (2001b).

For illustration, the flow pattern, represented by the instantaneous free vortices positions is presented in Fig. 2; this flow refers to case for $l/b=4$ and $\alpha=45^\circ$. The results of the mean drag coefficient and mean lift coefficient for $l/b=4$ at $\alpha=45^\circ$ obtained in the present simulation (Alcântara Pereira and Hirata, 2006b) are presented in Table 3. In this table one can find also experimental (Lam and Fang, 1995) and numerical results Lam *et al.* (2001a). The numerical results of Lam *et al.* (2001a) were also obtained using the Vortex Method where surface of the each cylinder was represented by straight-line panels with a point vortex located at the control point and the pressure on the airfoil surface was calculated according to the inviscid flow analysis.

As one can see, the agreement between the two numerical methods is very good for the mean drag coefficient and both results are close to the experimental values. However, as mentioned earlier, the three-dimensional effects present in the experiments are very important for the Reynolds number used in the simulations. Therefore a purely two-dimensional computation of such flow must produce higher values for the drag coefficient, as obtained for our simulation. Lam and Fang (1995) do not furnish results for the Strouhal numbers.

Table 3. Comparison of the mean drag coefficient and lift coefficient for $l/b=4$ and $\alpha=45^\circ$, for $Re=1.3 \times 10^4$.

Results	l/b	Cylinder 1	Cylinder 2	Cylinder 3	Cylinder 4
$\overline{C_D^+}$	4.0	1.02	1.3	0.62	1.3
$\overline{C_D^*}$	4.0	1.06	1.1	0.5	1.29
$\overline{C_D^\circ}$	4.0	1.22	1.27	0.83	1.26
$\overline{C_L^+}$	4.0	-0.01	-0.02	-0.02	-0.03
$\overline{C_L^*}$	4.0	-0.14	-0.15	-0.13	-0.16
$\overline{C_L^\circ}$	4.0	-0.07	-0.09	-0.12	-0.14

⁺ Experimental results (Lam and Fang, 1995)

^{*} Numerical results (Lam *et al.*, 2001a)

[°] Present simulation without turbulence model

The results of this analysis, taking into account the sub-grid turbulence modeling are presented in Table 4.

Table 4. Comparison of the mean drag coefficient and lift coefficient for $l/b=4$ and $\alpha=45^\circ$, for $Re=1.3 \times 10^4$.

Results	l/b	Cylinder 1	Cylinder 2	Cylinder 3	Cylinder 4
$\overline{C_D^+}$	4.0	1.02	1.3	0.62	1.3
$\overline{C_D^*}$	4.0	1.06	1.1	0.5	1.29
$\overline{C_D^\circ}$	4.0	1.23	1.29	0.86	1.27
$\overline{C_L^+}$	4.0	-0.01	-0.02	-0.02	-0.03
$\overline{C_L^*}$	4.0	-0.14	-0.15	-0.13	-0.16
$\overline{C_L^\circ}$	4.0	-0.04	-0.06	-0.09	-0.11

⁺ Experimental results (Lam and Fang, 1995)

^{*} Numerical results (Lam *et al.*, 2001a)

[°] Present simulation with turbulence model

Figure 2 shows the position of the wake vortices for $l/b=4$ and $\alpha=45^\circ$ using turbulence modeling at last step of the computation ($t=60$), where we can clearly observe the formation and shedding of large eddies in the wakes. This process occurs alternately on the upper and lower surfaces of each cylinder arranged in square configuration. We can also visualize the vortex pairing process, where the vortices rotate in opposite directions and are connected to each other by a vortex sheet. The separation phenomenon associated with the existence of adverse pressure gradients on the surface of the upstream and downstream cylinders occurs alternately on the top and bottom surfaces. Hence separation takes place in the laminar mode as experimentally expected for a sub-critical Reynolds number forming free shear layers. An immediate transition to turbulence close to the cylinder is observed accompanied by a very short recirculation region. Compared with the low Reynolds number case, transition to turbulence moves farther upstream.



Figure 2. Position of the wakes vortices at $t=60$ for $l/b=4$, $\alpha=45^\circ$, $Re=1.3 \times 10^4$, $\epsilon=\sigma_0=0.03b$, $\Delta t=0.05$, $M=50$.

Finally the sub-grid turbulence modeling is of significant importance for the numerical simulation, especially for flow around bluff bodies (Alcântara Pereira *et al.*, 2002), and a necessary step for the roughness modeling, which is in preparation to be presented elsewhere.

5. Conclusions

In the present study, a methodology for the numerical simulation of a viscous turbulent was employed (Alcântara Pereira *et al.*, 2002), where the large structures of the flow are described using a cloud of discrete Lamb vortices, which is used to simulate the vorticity present in the fluid region. In order to take into account the smaller scale manifestations of the flow and still keeping the computational effort within a manageable range, a second-order velocity structure function model was adapted to the Lagrangian scheme. This methodology has been used to simulate the flow around a cascade of NACA 65-410 airfoils (Alcântara Pereira *et al.*, 2004).

Some discrepancies observed in the determination of the aerodynamics loads may be also attributed to errors in the treatment of vortex element moving away from a solid surface. Because every vortex element has different strength of vorticity, it will diffuse to different location in the flow field. It seems impossible that every vortex element will move to same ϵ -layer normal to the solid surface. In the present method all nascent vortices were placed into the cloud through a displacement $\epsilon=\sigma_0=0.03b$ normal to the panels.

In order to ensure a more wide application, several additional testes with different gap distances, number of circular cylinders, and Reynolds number would be needed.

The use of a fast summation scheme to determine the vortex-induced velocity, such as the Multiple Expansion scheme, allows an increase in the number of vortices and a reduction of the time step, which increases the resolution of

the simulation, in addition to a reduction of the CPU time, which allows a longer simulation time to be carried out. The present calculation required 22 h of CPU time in an Intel(R) Pentium(R) 4 CPU 1700 MHz.

Finally, two aspects will be incorporated in this present study: vortex formation in the wake of a group of oscillating cylinders (Williamson and Roshko, 1988; Recicar *et al.*, 2006; Moura *et al.*, 2006) and heat-fluid motion handling the natural convection with the vortex created by the buoyancy that is caused by the heat (Ghoniem *et al.*, 1988; Ghoniem and Sherman, 1985; Ogami, 2001; Alcântara Pereira and Hirata, 2003).

6. Acknowledgements

The authors would like to acknowledge FAPEMIG (Proc. TEC-748/04) for the financial support during the time of this project.

7. References

- Alam, M. M., Moriya, M., Takai, K. and Sakamoto, 2003, "Fluctuating Fluid Forces Acting on Two Circular Cylinders in a Tandem Arrangement at a Subcritical Reynolds Number", *J. Wind Eng. Ind Aerodyn.*, 91, pp. 139-154.
- Alcântara Pereira, L.A. and Hirata, M.H., 2006a, "The Effects of Interference between Two Circular Cylinders Arranged in Tandem by Vortex Method Using Turbulence Modeling", 11th Brazilian Congress of Thermal Sciences and Engineering, Proceedings of ENCIT 2006, December 5-8, Curitiba, Brazil.
- Alcântara Pereira, L.A. and Hirata, M.H., 2006b, "On Interference between Circular Cylinders in Cross Flow at High Reynolds Number Using Surface Vorticity Method", 11th Brazilian Congress of Thermal Sciences and Engineering, Proceedings of ENCIT 2006, December 5-8, Curitiba, Brazil.
- Alcântara Pereira, L.A., Hirata, M.H. and Manzaneres Filho, N. 2004, "Wake and Aerodynamics Loads in Multiple Bodies - Application to Turbomachinery Blade Rows", *J. Wind Eng. Ind Aerodyn.*, 92, pp. 477-491.
- Alcântara Pereira, L.A. and Hirata, M.H. 2003, "Heat Transfer in the Wake Behind a Body Using A Particle Method", 17th International Congress of Mechanical Engineering, Proceedings of COBEM 2003, November 10-14, São Paulo, SP, Brazil.
- Alcântara Pereira, L.A., Ricci, J.E.R., Hirata, M.H. and Silveira-Neto, A., 2002, "Simulation of Vortex-Shedding Flow about a Circular Cylinder with Turbulence Modeling", *Intern'l Society of CFD*, Vol. 11, No. 3, October, pp. 315-322.
- Arie, M., Kiya, M., Moriya, M. and Mori, H., 1983, "Pressure Fluctuations on the Surface of Two Circular Cylinders in Tandem Arrangement", *ASME J. Fluids Eng.* 105, pp. 161-167.
- Batchelor, G.K. , 1967, "An Introduction to Fluid Dynamics", Cambridge University Press, Cambridge, UK.
- Biermann, D. and Herrnstein, Jr., 1933, "The Interference between Struts in Various Combinations", National Advisory Committee for Aeronautics, Technical Report 468.
- Chorin, A.J., 1973, "Numerical Study of Slightly Viscous Flow", *Journal of Fluid Mechanics*, Vol. 57, pp. 785-796.
- Ferziger, J.H., 1981, "Numerical Methods for Engineering Application", John Wiley & Sons, Inc.
- Ghoniem, A.F., Heidarinejad, G. and Krishan, A., 1988, "Numerical Simulation of a Thermally Stratified Shear Layer Using the Vortex Element Method ", *J. Comp. Physics.*, Vol. 79, pp. 135-166.
- Ghoniem, A.F. and Sherman, F.S., 1985, "Grid-Free Simulation of Diffusion Using Randon Walk Methods", *J. Comp. Physics*, Vol. 61, pp. 1-37.
- He, F. and Su, T.C., 1998, "A Numerical Study of Bluff Body Aerodynamics in High Reynolds Number Flows by Viscous Vortex Element Method", *J. Wind Eng. Ind. Aerodyn.*, 77/88, pp. 393-407.
- Hiwada, M., Mabuchi, I. and Yanagihara, H., 1982, "Flow and Heat Transfer from Two same Size Circular Cylinders in Tandem Arrangement" (In Japanese), *Trans. JSME* 48, pp. 499-508.
- Igarashi, T., 1984, "Characteristics of the Flow Around Two Circular Cylinders Arranged in Tandem", (Second Report), *Bull. JSME* 27 (233), pp. 2380-2387.
- Igarashi, T., 1981, "Characteristics of the Flow Around Two Circular Cylinders Arranged in Tandem", (First Report), *Bull. JSME* 24 (188), pp. 323-331.
- Jendrzeczk, J.A. and Chen, S.S., 1986, "Fluid Forces on Two Circular Cylinders in Cross Flow", *ASME, PVP* 14, pp. 141-143.
- Kamemoto, K., 2004, "On Contribution of Advanced Vortex Element Methods Toward Virtual Reality of Unsteady Vortical Flows in the New Generation of CFD", Proceedings of the 10th Brazilian Congress of Thermal Sciences and Engineering-ENCIT 2004, Rio de Janeiro, Brazil, Nov. 29 - Dec. 03, Invited Lecture-CIT04-IL04.
- Kamemoto, K., 1994, "Development of the Vortex Methods for Grid-Free Lagrangian Direct Numerical Simulation". *Proc. Third JSME-KSME*, Sendai, Japan, pp. 542-547.
- Kamemoto, K., 1993, "Procedure to Estimate Unstead Pressure Distribution for Vortex Method" (In Japanese), *Trans. Jpn. Soc. Mech. Eng.*, Vol. 59, No. 568 B, pp. 3708-3713.
- Kareem, A., Kijewski, T. and Po-Chien, L., "Investigation of Interference Effects for a Group of Finite Cylinders", 1998, *J. Wind Eng. Ind. Aerodyn.* 77&78, pp. 503-520.

- Kostic, Z.G. and Oka, .S.N, 1972, "Fluid Flow and Heat Transfer with Two Circular Cylinders in Cross Flow", *Int. J. Heat Mass Transfer*, 15, pp. 279-299.
- Lam, K., So, R.M.C. and Li, J.Y., 2001a, "Flow Around Four Cylinders in a Square Configurations Using Surface Vorticity Method", *Proceedings of The Second International Conference on Vortex Methods*, September 26-28, Istanbul, Turkey.
- Lam, K., Chan, K.T., So, R.M.C. and Li, J.Y., 2001b, "Velocity Map and Flow Pattern of Flow around Four Cylinders in a Square Configuration at Low Reynolds Number and Large Spacing Ratio Using Particle Image Velocimetry", *Proceedings of The Second International Conference on Vortex Methods*, September 26-28, Istanbul, Turkey.
- Lam, K. and Fang, X., 1995, "The Effect of Interference of Four Equal-Distance Cylinders in Cross Flow on Pressure and Forces Coefficients", *Journal of Fluid Structures*, Vol. 9, pp. 195-214.
- Lam, K. and Lo, S.C., 1992, "A Visualization Study of Cross-Flow around Four Cylinders in a Square Configuration", *Journal of Fluids and Structure*, Vol. 6, pp. 109-131.
- Lesieur, M. and Métais, O., 1996, "Spectral Large-Eddy Simulations of Isotropic and Stably-Stratified Turbulence", *An. Rev. in Fluid Mech.*, Vol. 28, pp. 45-82.
- Lewis, R.I., 1999, "Vortex Element Methods, the Most Natural Approach to Flow Simulation - A Review of Methodology with Applications", *Proceedings of 1st Int. Conference on Vortex Methods*, Kobe, Nov. 4-5, pp. 1-15.
- Métais, O. and Lesieur, M., 1992, "Spectral Large-Eddy Simulations of Isotropic and Stably-Stratified Turbulence", *J. Fluid Mech.*, Vol. 239, pp. 157-194.
- Moura, W.H., Alcântara Pereira, L.A. and Hirata, M.H., 2006, "Analysis of the Flow Around an Oscillating Circular Cylinder in Ground Effect", *11th Brazilian Congress of Thermal Sciences and Engineering*, *Proceedings of ENCIT 2006*, December 5-8, Curitiba, Brazil.
- Mustto, A.A., Hirata, M.H. and Bodstein, G.C.R., 1998, "Discrete Vortex Method Simulation of the Flow Around a Circular Cylinder with and without Rotation", *A.I.A.A. Paper 98-2409*, *Proceedings of the 16th A.I.A.A. Applied Aerodynamics Conference*, Albuquerque, NM, USA, June.
- Novak, J., 1974, "Strouhal Number of a Quadrangular Prism, Angle Iron and Two Circular Cylinders Arranged in Tandem", *Acta Tech. CSAV* 19 (3), pp. 361-373.
- Ogami, Y., 2001, "Simulation of Heat-Fluid Motion by the Vortex Method", *J.S.M.E. International Journal, Series B*, Vol. 44, No. 4, pp. 513-519.
- Ohya, Y., Okajima, A. and Hayashi, M., 1989, "Wake Interference and Vortex Shedding", In: *Encyclopedia of Fluid Mechanics*, Chap. 10 (Gulf Publishing, Houston, 1989).
- Okajima, A., 1979, "Flow Around Two Tandem Circular Cylinders at very High Reynolds Numbers", *Bull. JSME* 22 (166), pp. 504-511.
- Recicar, J.N., Alcântara Pereira, L.A. and Hirata, M.H., 2006, "Harmonic Oscillations of a Circular Cylinder Moving with Constant Velocity in a Quiescent Fluid", *11th Brazilian Congress of Thermal Sciences and Engineering*, *Proceedings of ENCIT 2006*, December 5-8, Curitiba, Brazil.
- Sarpkaya, T., 1989, "Computational Methods with Vortices - The 1988 Freeman Scholar Lecture", *Journal of Fluids Engineering*, Vol. 111, pp. 5-52.
- Sethian, J.I., 1991, "A Brief Overview of Vortex Method, Vortex Methods and Vortex Motion", *SIAM*. Philadelphia, pp. 1-32.
- Shintani, M. and Akamatsu, T., 1994, "Investigation of Two Dimensional Discrete Vortex Method with Viscous Diffusion Model", *Computational Fluid Dynamics Journal*, Vol. 3, No. 2, pp. 237-254.
- Smagorinsky, J., 1963, "General Circulation Experiments With the Primitive Equations", *Mon. Weather Rev.*, Vol. 91, pp. 99-164.
- Teixeira da Silveira, L., Alcântara Pereira, L.A. and Hirata, M.H., 2005, "The Effects of Interference between Two Circular Cylinders Arranged in Tandem by Vortex Method", *18th International Congress of Mechanical Engineering*, *Proceedings of COBEM 2005*, November 6-11, Ouro Preto, MG.
- Uhlman, J.S., 1992, "An Integral Equation Formulation of the Equation of an Incompressible Fluid", *Naval Undersea Warfare Center*, T.R. 10-086.
- Williamson, C.H.K. and Roshko, A., 1988, "Vortex Formation in the Wake of an Oscillating Cylinder", *J. Fluids and Structures*, Vol. 2, pp. 239-381.
- Zdravkovich, M.M., 1977, "Review of Flow Interference between Two Circular Cylinders in Various Arrangements", *Trans. SAME, J. Fluid. Eng.*, 99, pp. 618-633.
- Zdravkovich, M.M. and Pridden, D.L., 1977, "Interference between Two Circular Cylinders; Series of Unexpected Discontinuities", *J. Ind. Aerodyn.* 2, pp. 255-270.
- Zdravkovich, M.M. and Pridden, D.L., 1975, "Flow Around Two Circular Cylinders", *Research Report*, *Proceedings of the Second US National Conference on Wind Engineering Research*, Fort Collins, IV (18).

8. Responsibility notice

The authors are the only responsible for the printed material included in this paper.